VALIDITY OF J ESTIMATION IN PIPING COMPONENTS BASED ON R6/3 OPTION 2 K_r - L_r RELATIONSHIP

Ph. GILLES*, A. PELLISSIER TANON*, C. FRANCO*, J. VAGNER*

The R6/3 option 2 K_r - L_r relationship provides a convenient way to determine an approximate value of J in a non-linear material from the elasticity computed value J^e. The K_r-L_r relationship depends only on the material stress-strain curve, therefore the determination of L_r leads to the K_r value and J is given by the ration J^e/K_r. This paper examines the conditions ensuring the validity of such an approach and presents four examples of application to surface cracked components.

INTRODUCTION

In nuclear power plants, most of safety analyses require parametric defect assessment studies in components subjected to several types of loadings. Due to the high level of the considered loadings under faulted condition, or of thermal shock loadings in some operational conditions, one has to consider the non linear behaviour of the materials. The analyses are generally performed using simplified methods which estimate J from the Stress Intensity Factors (SIFs) of the elastic solution through a plasticity correction.

EDF+ , CEA# and FRAMATOME* have therefore developed a substantial effort over a number of years to establish and validate simplified Fracture Mechanics methods. Among currently used methods, the R6/3 option 2 approach developed by Ainsworth (1), and incorporated in the revision 3 of the R6 procedure (2), offers a very convenient way of deriving the plasticity correction. This method, validated on two-dimensional cracked geometries, has been applied to three dimensional cracked structures like plates, pipes (3,4,5,6) and more recently tees (7).

* FRAMATOME, Tour FIAT, 92084 PARIS-LA-DEFENSE, FRANCE.
+ French utility "Electricité de France"
# French atomic energy commission "Commissariat à l'Energie Atomique"

The key issue for the applicability of the method is the existence of the scaling parameter L_T and the determination of the reference load which defines L_T. The analysis of several recent experimental and numerical results enables clarification of the definition of this reference load. In the four three dimensional (3D) cases presented in this paper, the J values obtained through the R6/3 option 2 method, with properly defined reference loads, are very close to the J values obtained by numerical elastic-plastic computations.

DEFINITION OF J AND EXAMINATION OF THE BASES OF J ESTIMATION SCHEMES

Definition of the fracture parameter J in non linear elastic three dimensional structures

In two-dimensional cases, J. Rice (8) demonstrated that the rate of decrease of the potential energy per unit of crack length could be represented as a path-independent integral J.

This definition still holds for three dimensional structures under thermo-mechanical loading :

$$J = -\frac{\partial \Pi}{\partial A} \qquad (1)$$

where $\Pi = \Psi - W$ is the potential energy
Ψ is the free energy and W the work of the external forces.
A is the cracked area.
The derivative of Π is considered with respect to a crack extension which has to be tangent to the crack. This extension may be local, giving a local J, or correspond to a global change of the crack shape.

Rice's path independent integral has been extended to 3D cases by Destuynder (9) and de Lorenzi (10). Both proposed equivalent formulations of domain integrals. The numerical results presented in this paper have been obtained using the G-θ method (9).

Under an applied displacement q and a purely mechanical loading, we get :

$$J = -\int_0^q \left.\frac{\partial Q}{\partial A}\right|_q dq \qquad (2)$$

where Q is the reaction force

Extension of the definition of J to elastic-plastic fields

For a non-linear elastic material, a relationship between J and the amplitude of the singular fields has been evidenced by Hutchinson, Rice and Rosengren, but only in the 2D case (the HRR field). These results are only valid in the frame of the J2 Deformation Plasticity Theory (D.P.T.(11)) which may be used to describe the plastic behaviour of a body under the following assumptions:

_ isotropic behaviour,
_ incompressibility (in full plasticity),
_ loading depends on only one parameter and increases monotonically,
_ tensile behaviour is described by a power law,
_ plastic behaviour obeys the Prandtl's stress-strain laws,
_ elastic strains are small compared to the plastic ones.

For a monotonically increasing proportional loading, the differences between incremental elastic-plastic theory and DPT are small, in 2D and 3D cases, provided the stress-strain law is also monotonic. The demonstration showing that J defined by (1) is suitable to describe the initiation of ductile tearing, and to analyse stable and unstable ductile crack growth, rests on the assumption of the dominance of the HRR field. An analysis of the applicability of this definition of J to 3D conditions is given in (12).

This paper does not consider the question of the validity of J defined by (1), as a fracture criterion. It only examines the validity and accuracy of the R6/3 option 2 approach as a simplified method to estimate J in 3D configurations.

Fundamental assumptions of the J estimation schemes

All the J-estimation schemes are based on the DPT hypotheses. Moreover, they assume that the elastoplastic response of the body is given by the superposition of the elastic and fully plastic solutions :

$$q = q^e + q^p \quad \Rightarrow \quad J = J^e + J^p \qquad (3)$$

Shih demonstrated this equation to be exact for a two-dimensional plate under shear loading. Generally, this is only an approximation, so that J is obtained comprising a plastic correction on the elastic term (13) :

$$J = J^{ec} + J^p \qquad (4)$$

The J^e term is obtained from SIF analytical or tabulated solutions.
The J^{ec} is the J^e value for an adjusted crack length given by:
$a^e = a + \Phi r_y$ where a is the crack length, r_y Irwin's plastic zone correction and Φ an adjustment factor chosen as $1/(1 + (Q / Q_0)^2)$, the scaling load Q_0 being defined hereafter.

Derivation of the plastic component of J

Illyushin has shown (11) that in DPT the load-displacement relationship takes the same form as the stress-strain law:

$$\varepsilon^p = \varepsilon_0 \left(\frac{\sigma}{\sigma_0}\right)^n \quad \Rightarrow \quad q^p = \varepsilon_0 \, L(A,n) \left(\frac{Q}{Q_0}\right)^n \tag{5}$$

where $Q_0 = \sigma_0 \, g_0(A,n)$ is an arbitrary scaling load.

(5) may be written as:

$$Q = Q_0 \left(\frac{1}{L}\right)^{1/n} \left(\frac{q^p}{\varepsilon_0}\right)^{1/n} = \sigma_0 \, g(A,n) \, h(q^p, n) \tag{6}$$

with $$g = g_0 \left(\frac{1}{L}\right)^{1/n} \; ; \; h = \left(\frac{q^p}{\varepsilon_0}\right)^{1/n} \tag{6'}$$

showing the separability of geometric and load variables.

From (2) we get :

$$J^p = -\frac{g'}{g} \int_0^{q^p} Q \, dq^p = \eta \frac{U^p}{S} \tag{7}$$

where g' is the derivative of g with respect to a crack size parameter corresponding to a given crack shape and pattern of crack extension

U is the strain energy and S is a scaling area

The η factor is a non-dimensional function of the cracked geometry and the hardening exponent n.

<u>Derivation of the R6/3 option 2 method</u>

This method leads to a J formula which depends on the material properties only through the stress-strain law. This avoids any fitting of the stress-strain curve. The method allows derivation of J from J^e through a plasticity correction K_r, which is a function of the stress-strain law and the load to reference load ratio L_r. Reference loads have to be defined for each type of geometry and loading.

$$J = \frac{J^e}{\left[K_r(L_r)\right]^2} \tag{8}$$

Owing to the fundamental part played by the reference load, this method is also called the reference load approach.

This method has been developed by Ainsworth (1) using the GE-EPRI results (13). The approach derives from the above mentioned basic relationships, as shown in the following. Considering the load-displacement equation (5) and the J^p formula (7), we get

$$J^p = \sigma_0 \, \varepsilon_0 \frac{n}{n+1} (-g') \, L^{\frac{n+1}{n}} \left(\frac{Q}{Q_0}\right)^{n+1} \tag{9}$$

which has the same form as the basic GE-EPRI (13) formula:

$$J^p = \sigma_0 \varepsilon_0 B h_{1n} \left(\frac{Q}{Q_0}\right)^{n+1} \quad \text{with} \quad h_{1n} = h_1(A,n) \quad (10)$$

Ainsworth simplifies and generalises the GE-EPRI expressions by making four supplementary hypotheses (H1,H2,H3,H4).

The h_{1n} values depends on Q_0, but H1 hypothesis assumes that an appropriate selection of Q_0 can make h_{1n} independent of n according to:

(H1) $h_{1n} = h_{1ref} \left(\frac{Q_0}{Q_{ref}}\right)^{n+1}$ (11), where h_{1ref} depends only on the geometry.

This allows us to write:

$$J^p = B\, h_{1ref} \sigma_{ref}\, \varepsilon^p_{ref} \quad (12)$$

where

$$\sigma_{ref} = \sigma_0 \frac{Q}{Q_{ref}} \quad (13)$$

and ε^p_{ref} is the corresponding plastic strain on the material curve.

The second hypothesis (H2) consists in the generalisation of these results to any type of stress-strain law.

For a linear behaviour:

$J^e = \mu\, B\, h_{11} \frac{\sigma^2_{ref}}{E}$ with $\mu = \frac{1-\nu^2}{.75}$ in Plane Strain or $\mu = 1$ in Plane Stress.

Using the GE-EPRI plastic zone correction, we get: $J^{ec} \cong J^e \left(1 + \Phi \frac{r_y}{a}\right)$

Therefore:

$$\frac{J}{J^e} = 1 + \Phi \frac{r_y}{a} + \frac{h_{1ref}}{\mu\, h_{11}} \left(\frac{E\varepsilon_{ref}}{\sigma_{ref}} - 1\right)$$

where $\varepsilon_{ref} = \frac{\sigma_{ref}}{E} + \varepsilon^p_{ref}$ is the total strain.

The H3 hypothesis consists in the assumption that $h_{1ref} = \mu\, h_{11}$.

Then, Ainsworth rewrites the plastic zone correction and obtains the relationship :

$$K_r = \sqrt{\frac{J^e}{J}} = \left[\frac{L_r^2}{2\left(1+L_r^2\right)} + \frac{E\,\varepsilon_{ref}}{\sigma_{ref}}\right]^{-\frac{1}{2}} \quad (14)$$

The R6/3 document (2) uses another plastic zone correction, which gives slightly different K_r values:

$$K_r = \sqrt{\frac{J^e}{J}} = \left[\frac{L_r^2\, \sigma_{ref}}{2E\,\varepsilon_{ref}} + \frac{E\,\varepsilon_{ref}}{\sigma_{ref}}\right]^{-\frac{1}{2}} \quad (14')$$

Lastly, Ainsworth takes the yield limit load as the reference load. This constitutes the (H4) hypothesis which will be discussed in the next paragraph.

DISCUSSION OF THE SIGNIFICANCE OF THE REFERENCE LOAD APPROACH

It is suggested in (12) that the structure of the load-displacement relationship (6), in which the crack geometry parameters and the displacement are separated variables, implies that the plastic strain field follows a well defined pattern for a large range of load level and crack size. The proposal is also true in reverse. Such an overall deformation mechanism ensures the applicability of the DPT. Reference (12) derives very strong experimental and analytical evidence of this behaviour from experiments conducted on austenitic through-wall cracked pipes under bending (14).

In a Rigid Perfectly Plastic material, this pattern is the kinematic deformation field (the slip-line field in 2D conditions) corresponding to the limit load. In a strain hardening material, under a proportional loading, the same type of deformation pattern exists but the strain localises in shear bands instead of slip lines.

These remarks lead us to consider that the reference load should be defined as the load above which the plastic strain field presents that specific pattern. This load is the yield limit load based on the material conventional yield stress computed over the area where the overall deformation mechanism develops (e.g. a plastic hinge in the cracked section or the collapse of a short ligament). In a 2D structure, it is logical to associate this load with the full yield of the cracked cross section. This state can unambiguously be defined in the deep crack situation, when the plastic zone grows from the crack tip towards the opposite free surface. So, the reference load may be obtained through a classical numerical elastic-plastic analysis of the structure.

A more general definition of the reference load, namely applicable to 3D cases and experiments, may be obtained by considering the load-displacement curve describing the overall deformation mechanism (e.g. the moment-ovalisation for a longitudinal crack in an elbow subjected to bending). Obviously, the specific plastic strain pattern is established when the non-linear part of this displacement overcomes the linear one. The transition corresponds to the load at which these two parts of the displacement are equal and defines the reference load.

For shallow cracks for which the plastic pattern may vary quite widely with the amount of strain hardening, a pseudo reference load may be found only in a restricted range of strain hardening values.

KJ FORMULAE IN FOUR NON-LINEAR 3D STRUCTURES

In all the considered cases, the same procedure has been applied: $K_r = \sqrt{J^e/J}$ is computed numerically (R6 option 3) and through equation (14) (R6 option 2) using

analytical or computed estimates of the reference load. Both values are plotted as a function of L_r. The variations of the plasticity correction along the crack front are illustrated by plots of $J/J_{Deepest\ Point}$ versus angular position (Shape Curves). The main geometrical parameters are: the internal and mean radius R_i and R_m of the section, r the elbow curvature radius and t the thickness.
All the cracks have a semi-elliptical shape defined by the depth over the length ratio a/c. Their size is characterised by the depth over the thickness ratio a/t. The mesh elements are isoparametric and quadratic. The plasticity model is the Von Misès isotropic criterion. All the computations are conducted under the large displacement hypothesis. The first case is analysed with FRAMATOME's SYSTUS Finite-Element code, the other with CASTEM2000 developed by C.E.A..

Pressurised pipe with a longitudinal external crack

The crack is long (a/c = .190) and deep (a/t = .712). The model simulates a burst test, and a good correlation with the experiment has been obtained (15), owing to the high degree of mesh refinement. The local bulging of the cracked area represents the deformation mechanism. The reference load expression is derived from Battelle's empirical formula (16) but needs further validation for a range of M values.

$$L_r = \frac{p\,R_i/t}{\sigma_y}\,\frac{A_0 - A/M}{A_0 - A} \qquad (15)$$

where $A_0 = 2(c+t)\,t$ and $A = \pi\,a\,c$ represents the cracked area

M is the bulging factor given by Krenk's formula

$$M = .614 + .481\lambda_k + .386\,e^{-1.25\lambda_k} \qquad (16)$$

with $\lambda_k = \left[12\left(1-\nu^2\right)\right]^{.25} c/\sqrt{R\,t}$

The agreement between option 3 and 2 curves is good but the computation has been conducted only up to the initiation load (Fig. 1). The shape curves are almost identical except in the very close vicinity to the free surface (Fig. 2).

Pipe with a circumferential external crack under pure bending

The crack is rather short (a/c=.5) and shallow (a/t = .25). The mesh is refined around the crack and contains more than 6200 nodes. Here the development of the plastic pattern is controlled by the rotation of the cracked pipe section around the neutral axis. The reference load is given by the global limit load of the cracked section (Wilkowski's formula) :

$$Q_{ref}^{PCib} = 4\sigma_y R^2\,t\,\left(\cos\left(\gamma\frac{a}{2t}\right) - .5\frac{a}{t}\sin\gamma\right) \text{ with } \gamma = \frac{c}{R_e} \qquad (17)$$

The agreement between option 3 and 2 curves is excellent up to L_r = 1.5 (Fig. 3). The shape curves are close to each other except at the vicinity of the free surface(Fig. 4).

Elbow with a circumferential external crack under pure bending

The crack is the same as is the second case and the mesh is identical. The mechanism controlling the plastic deformation is the same as in the pipe. The reference load is given by the global limit load of the cracked section deduced from Calladine's formula (17) :

$$Q_{ref}^{ECib} = .88\,\lambda^{2/3}\; Q_{ref}^{PCib} \qquad \text{with} \quad \lambda = \frac{r\,t}{R^2} \qquad (18)$$

The agreement between option 3 and 2 curves is excellent up to $L_r = 1.4$ (Fig. 5). The shape curves are close to each other except at the vicinity of the free surface (Fig. 6).

Elbow with a longitudinal external crack under bending

This case corresponds to an experiment conducted on an elbow subjected to a variable closing moment and a compressive load. The ovalisation induced by the formation of axial hinges on the crown is the controlling mechanism of plastic deformation. Due to the elbow curvature, this mechanism is strongly connected to the rotation of the circumferential sections. The large displacement computations yield very good results compared to the measurements (18). The reference load is given by Griffith's formula (19) and corresponds to the excessive load measurement on the moment-ovalisation curve (Fig. 8). For the considered crack depth, the formula is identical to (18). The estimation scheme gives a conservative value of J up to $L_r = 1.1$. The proposed L_r formula is not very accurate since the influence of the tranverse and axial loads on the yielding is not considered. Again, the shape curves are very close to each other except near the free surface where the stress triaxiality differs greatly from the plane strain state which dominates along more than eighty percent of the crack front.

This closeness of the shape curves, shows that, under proportional loading, the amplification factor to the elastically computed J due to yielding does not depend on the local stress level but on a the global load. This justifies the reference load model.

CONCLUSION

The R6 option 2 procedure may be used to predict J from the elastically computed value J^e along the whole crack front. In 3D cases, the bases of this approach are clarified and four examples show the accuracy of such a method.

REFERENCES

(1) Ainsworth, R.A. "The Assessment of defect in structures of strain hardening material", Engineering Fracture Mechanics, 19 (1984), 633-642.

(2) Milne, I., Ainsworth, R.A., Dowling, A.R., Stewart, A.T. "Assessment of the integrity of structures containing defects", R/H/R6 - rev. 3, CEGB, May 1986.

(3) Miller, A.G. "J estimation for surface defects", Report TPRD/B/O811/R86, Central Electricity Generating Board, 1986.

(4) Chell, G.G. "Application of the CEGB Failure Assessment Procedure, R6, to Surface Flaws", Research Report RD/L/3415/R88, Central Electricity Generating Board, January 1989.

(5) Franco, C. and Gilles, P. "Three-Dimensional Elastic-Plastic Analysis of Small Circumferential Surface Cracks in Pipes Subjected to Bending Load", Fracture Mechanics : Twenty-Second Symposium (Volume II), S.N. Atluri, J.C. Newman, Jr., I.S. Raju and J/S. Epstein, Eds., American Society for Testing and Materials, Philadelphia, 1992, pp. 183-205.

(6) Ignaccolo, S., Proix, J.M., Churier-Bossennec, H. and Faidy C., "3D Computation of Cracked Piping Components", PVP VOL.226, ASME 1993.

(7) Kristiansen, N.Ø., Turner, C.E. "Defect Assessment of Tubular T-Joints Using the R6 Failure Analysis Diagram", Journal of Pressure Vessel Technology, Vol. 115, November 1993, pp. 373-380.

(8) Rice, J.R. "Mathematical analysis in the mechanics of fracture" Fracture, and advanced treatise, tome 2, H. Liebowitz Ed., Acad. Press, 1968.

(9) Destuynder, Ph., Djaoua, M. "Sur une interprétation mathématique de l'intégrale de Rice en théorie de la rupture fragile", Mathematical Methods in Applied Sciences, 3, pp. 70-87, 1981.

(10) De Lorenzi, H.G. "3-D Elastic-Plastic fracture mechanics with Adina" Computers and Structures 13, pp. 613-621, 1981.

(11) Illyushin, A.A. "Plasticité - déformations élastoplastiques", Eyrolles, 1956.

(12) Pellissier-Tanon, A. "Mechanical bases and validation of the J resistance curve approach for large through-wall circumferential cracks in pipings". FRAMATOME Technical Report. Fratec 314 E, 01.07.1992

(13) Kumar, V., Shih, C.F. "Fully plastic crack Solution Estimation Scheme, and Stability Analyses for the Compact Specimen", Fracture Mechanics : Twelfth Conference, ASTM STP 700, pp. 406-438, American Society for Testing and Materials, 1980.

(14) Moulin, D., Lebey, J., Acker, D., "Experimental Determination of J Values on Circumferentially Cracked Stainless Steel Pipes under Bending", Proc. Conf. on Pipework Operation, I-Mech.E, 1989.

(15) Gilles, Ph., Mourgue, Ph., Rochette, M., "Précision du calcul de la force d'extension de fissure G : effets de maillage et avantages de la méthode G-θ ", Actes du Colloque National en Calcul des Structures, Ed; Hermès et INRIA, Paris, 1993, Vol.2, pp. 639-670.

(16) Kiefner, J.F., Maxey, W.A., Eiber, R.J., Duffy, A.R., "Progress in Flaw Growth and Fracture Toughness Testing", ASTM STP536 Failure Stress Levels of Flaws in Pressurized Cylinders, pp. 461-481, 1973.

(17) Calladine, C.R., J. Mech. Engng. Sci. 16 (2), 85, 1974.

(18) Gilles, Ph., Franco, Ch., Migné, C., "Numerical and Analytical of An Experiment Performed an a Longitudinally Cracked Elbow Subjected to In-plane Bending", To be submitted to the 26th National Symposium on Fracture Mechanics, July 1994.

(19) Griffiths, J.E., Int J. Mech. Sci., Vol. 21, pp. 119-130, 1979.

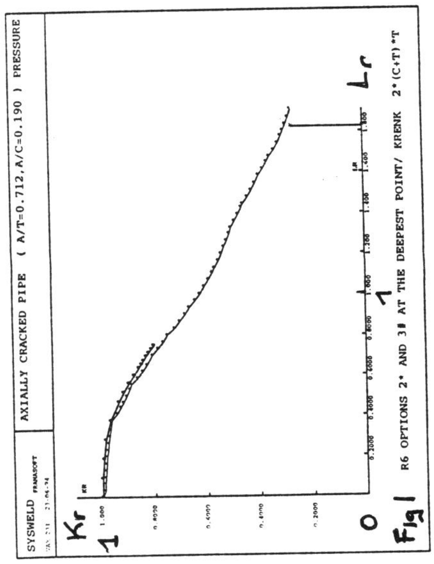
SYSWELD FRAMASOFT
AXIALLY CRACKED PIPE (A/T=0.712,A/C=0.190) PRESSURE
R6 OPTIONS 2* AND 3# AT THE DEEPEST POINT/ KRENK 2*(C+T)*T
Kr
Lr
Fig 1

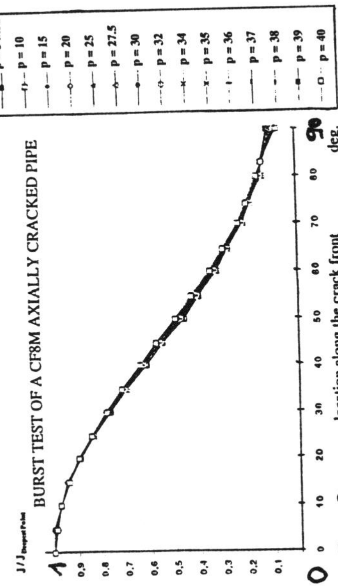
BURST TEST OF A CF8M AXIALLY CRACKED PIPE
location along the crack front
deg.
p = 5 MPa
p = 10
p = 15
p = 20
p = 25
p = 27.5
p = 30
p = 32
p = 34
p = 35
p = 36
p = 37
p = 38
p = 39
p = 40
Fig 2

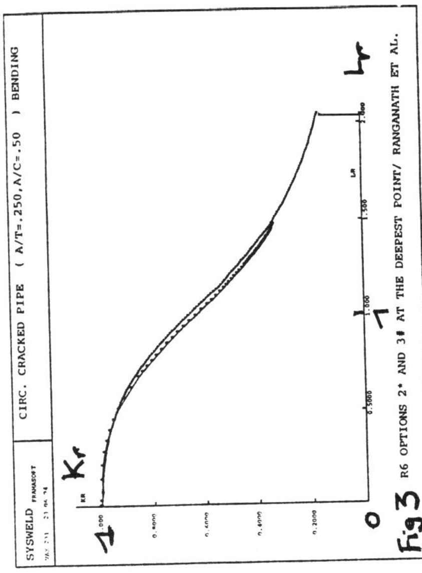
SYSWELD FRAMASOFT
CIRC. CRACKED PIPE (A/T=.250,A/C=.50) BENDING
R6 OPTIONS 2* AND 3# AT THE DEEPEST POINT/ RANGANATH ET AL.
Kr
Lr
Fig 3

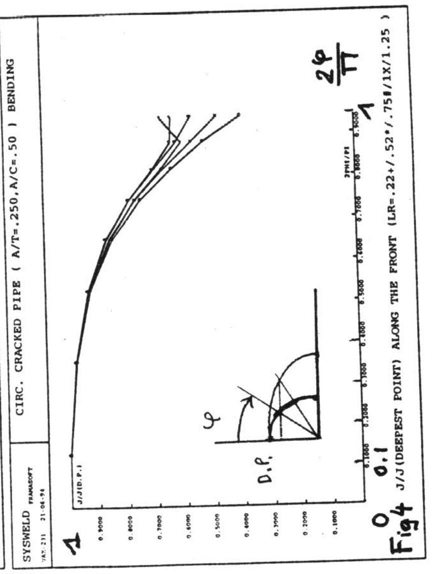
SYSWELD FRAMASOFT
CIRC. CRACKED PIPE (A/T=.250,A/C=.50) BENDING
J/J(DEEPEST POINT) ALONG THE FRONT (LR=.22+/.52*/.75#/1X/1.25)
D.P.
φ
2φ/π
Fig 4

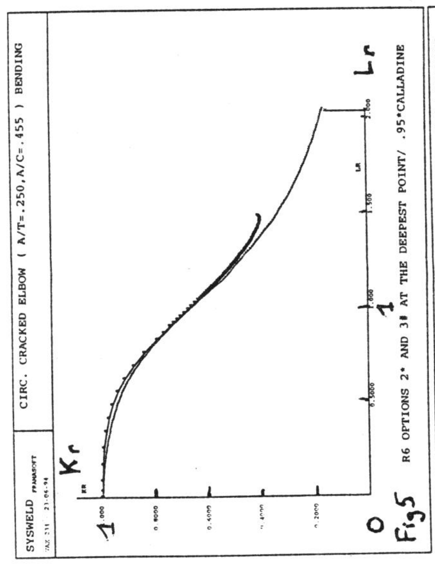
SYSWELD
CIRC. CRACKED ELBOW (A/T=.250,A/C=.455) BENDING
Kr
Lr
R6 OPTIONS 2* AND 3# AT THE DEEPEST POINT/ .95*CALLADINE
Fig5

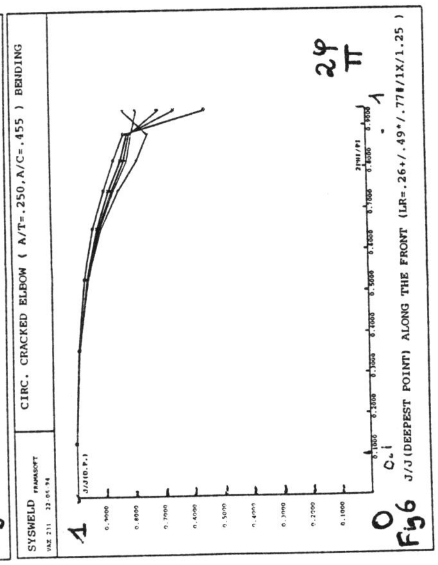
SYSWELD
CIRC. CRACKED ELBOW (A/T=.250,A/C=.455) BENDING
J/J(DEEPEST POINT) ALONG THE FRONT (LR=.26+/.49*/.77#/1X/1.25)
Fig6

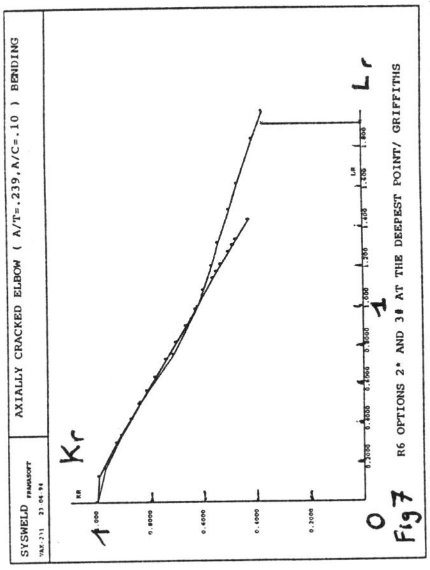
SYSWELD
AXIALLY CRACKED ELBOW (A/T=.239,A/C=.10) BENDING
Kr
Lr
R6 OPTIONS 2* AND 3# AT THE DEEPEST POINT/ GRIFFITHS
Fig7

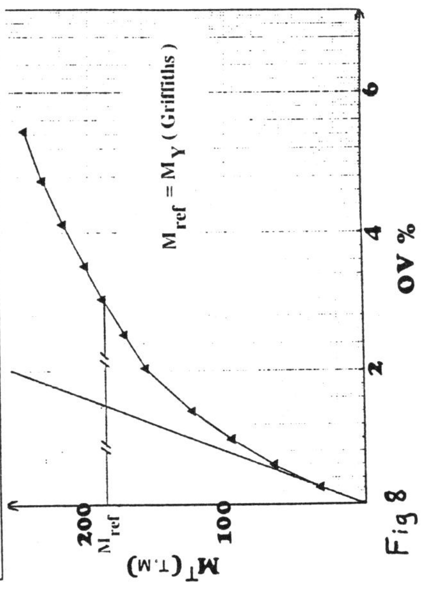
M_ref = M_Y (Griffiths)
OV %
M_T (T.M)
M_ref
Fig 8